

Supplement to “Cancer therapy shapes the fitness landscape of clonal hematopoiesis”

Supplementary Notes	2
References	6
Supplementary Figure 1. Quantification of the extent of natural selection by gene in clonal hematopoiesis using a dN/dS method	7
Supplementary Figure 2. Mutational characteristics of CH in 24,146 solid tumor patients.	8
Supplementary Figure 3. Relationship between variant allele fraction (VAF) and CH mutational features	9
Supplementary Figure 4. Relative odds of CH in specific genes by clinical characteristics	10
Supplementary Figure 5. Relationship between variant allele fraction (VAF) and <i>DNMT3A</i> mutations	11
Supplementary Figure 6. Mutational characteristics of CH in solid tumor patients and prior exposure to oncologic therapy	12
Supplementary Figure 7. Calculation of cumulative exposure for therapy subclasses.....	13
Supplementary Figure 8. Serial samples included in the study, of which at least one was analyzed by MSK-IMPACT.....	14
Supplementary Figure 9. Growth rate of CH mutations vs. mutation number	15
Supplementary Figure 10. Proportion of patients who gained or lost a mutation during follow-up period stratified by receipt of therapy	16
Supplementary Figure 11. Mutation landscape in tMN cases with at least one genetic alteration present at the time of tMN diagnosis	17
Supplementary Figure 12. Risk of myeloid malignancy by clinical and mutational characteristics comparing studies for tMN in solid tumor patients and AML risk in healthy individuals ..	18
Supplementary Figure 13. Precision of CH calling by simulation	19
Supplementary Figure 14. Recall of CH calling by simulation.....	20

Supplementary Notes for “*Cancer therapy shapes the fitness landscape of clonal hematopoiesis*”

Measurement of cumulative therapy dose

To define cumulative exposure to a therapeutic subclass of cytotoxic therapy, a simple sum of the mg/kg of drugs within a class cannot be used because drugs even within the same drug class are delivered on different dosing scales. To derive metrics for cumulative exposure to cytotoxic therapy subclasses, we applied the approach used by the Late Effects Study Group¹. For each drug the total dose per kg received prior to blood draw was summed for each patient. The dose distribution for each agent was divided into tertiles and the patient’s dose was assigned a score based on tertile of total exposure. An individual patient’s scores for each drug in a specific drug class were summed. The distribution of the resulting sum across all patients was used to derive tertiles of total exposure to the drug class in the entire cohort (Supplementary Figure 7).

Given the variety of radiotherapy fractionation schemes and prescribed tumor doses, we calculated the cumulative radiation dose received by each patient prior to blood draw in 2-Gy per fraction equivalents (EQD₂) using an α/β of 3 Gy, considering CH to be a late-responding tissue effect². We calculated tertiles of dose based on the distribution of cumulative EQD₂ received over the entire cohort and assigned each individual a score based on their tertile of exposure (*e.g.* a patient who did not receive external beam radiation received a score of zero for that particular agent. If the patient’s cumulative radiation dose, as expressed in EQD₂, was within the first tertile, a score of one was assigned, and so forth).

Clinical characteristics of previously published studies included in combined analyses

To study the relationships between CH and tMN we aggregated data from MSK with 5 previously published studies including Gillis et al. (MOF) Takahshi et al. (MDA), Gibson et al. (DFC), Young et al., (WSU) and Abelson et al. (EPI).

MOF

Gillis et al.³ performed a nested case-control study for tMN risk using subjects from an internal biorepository of 123,357 cancer patients who consented to participate in the Total Cancer Care biobanking protocol at Moffitt Cancer Center (Tampa, FL, USA) between Jan 1, 2006, and June 1, 2016. Cases were individuals diagnosed with a primary malignancy, treated with chemotherapy who subsequently developed a therapy-related myeloid neoplasm, and were 70 years or older at either diagnosis. Controls were individuals who were diagnosed with a primary malignancy at age 70 years or older and were treated with chemotherapy but did not develop therapy-related myeloid neoplasms. Controls were matched to cases in at least a 4:1 ratio on the basis of sex, primary tumour type, age at diagnosis, smoking status, chemotherapy drug class, and duration of follow-up. DNA was isolated from peripheral blood collected before therapy-related myeloid neoplasm diagnosis and subjected to Droplet-partitioned, targeted, amplicon-based, next-generation sequencing was used in accordance with the manufacturer's instructions (RainDance Technologies, Billerica, MA, USA) to identify somatic mutations in 49 myeloid-driver genes (ThunderBolts Myeloid Panel, RainDance, Billerica, MA, USA).

MDA

Takahashi et al.⁴ performed a case-control study for cancer patients who developed therapy-related myeloid neoplasms (cases) and lymphoma patients who did not develop therapy-related myeloid neoplasms (controls). Cases were identified using a clinical database at the Department of Leukemia of The University of Texas MD Anderson Cancer Center (Houston, TX, USA) including 40 000 patients who have consented for their data to be used in research. Inclusion criteria were that patients had to have been treated for a primary cancer from June 11, 1997, and subsequently had diagnoses of therapy-related myeloid neoplasms between Jan 1, 2003, and Dec 31, 2015, and had paired samples of diagnostic bone marrow at the time of therapy-related myeloid neoplasm diagnosis and peripheral blood samples obtained at the time of primary cancer diagnosis. An aged-matched control group (using a 3:1 control to case ratio) was identified using a clinical database of patients treated for lymphoma from 2008 to 2015. Eligible patients were those who had a pre-treatment blood sample available, had received a combination chemotherapy regimen including an alkylating agent, had at least 5 years of follow-up with no clinical evidence of therapy-related myeloid neoplasm development, and had no evidence of bone marrow metastasis of lymphoma in a bilateral bone marrow biopsy. Targeted sequencing of

32 myeloid genes was performed using an amplicon-based targeted deep sequencing method, including unique molecular barcodes.

DFC

Gibson et al.⁵ performed a cohort study among 401 adult patients who underwent ASCT for non-Hodgkin lymphoma between 2003 and 2010 (Dana-Farber Cancer Institute, Boston, MA; targeted sequencing cohort) with mobilized stem-cell products available at the time of ASCT. All subjects had been exposed to cancer therapy prior to stem cell collection. During the follow-up period 18 patients developed tMN. Targeted sequencing was performed using mobilized stem-cell products at the time of ASCT and on bone marrow aspirates obtained at the time of TMN diagnosis for all patients who had an available specimen (N=9). Targeted deep sequencing was performed using 86 known myeloid genes genes using the Custom SureSelect hybrid capture system (Agilent Technologies, Santa Clara, CA).

WSU

Young et al.⁶ utilized a nested case-control design for AML using data from two large cohort studies, the Nurses Health Study (NHS) and the Health Professionals Follow-Up Study. Subjects were drawn from the “blood sub-cohorts” of these two studies which included 32,826 women (NHS) with a blood sample from 1989-90 as well as 18,018 men (HPFS) who provided a whole blood sample from 1993-95. The case definition included all blood subcohort participants with confirmed diagnoses of AML (ICD-8=205.0) occurring after blood draw. Two matched controls were selected per case on cohort (sex), race, birthdate (± 1 year), and blood draw details (date ± 1 year, time ± 4 hours, fasting status $<8, 8+$ hours). In total this included 35 cases (16 NHS, 19 HPFS) and 70 controls (32 NHS, 38 HPFS). Samples were sequenced using the Illumina TruSight Myeloid Sequencing Panel for targeted capture from 54 leukemia-associated genes. Technical replicate libraries were sequenced on different machine runs. Error corrected sequencing analysis of raw sequencing results was performed as described elsewhere⁷.

EPI

Abelson et al.⁸ performed a case-control study for AML using samples from EPIC⁹. We used data from both the discovery and validation sets. The discovery set included 509 DNA samples from individuals who enrolled on the EPIC study between 1993 and 1998 across 17 different centres. This included 95 individuals who developed AML and 414 age- and gender-matched controls who did not develop any haematological disorders during the follow-up period. Subjects for the validation cohort were obtained from individuals enrolled in the EPIC-Norfolk longitudinal cohort study between 1994 and 2010. Samples were available from 37 patients with AML (of which 8 were already included in the discovery cohort) and 262 age- and gender-matched controls without a history of cancer or any haematological conditions. Targeted deep sequencing in the discovery cohort was performed using error-corrected, custom capture-based sequencing using the xGen AML Cancer Panel. Targeted sequencing in the validation set was performed using a custom complementary RNA bait set (SureSelect, Agilent, ELID 0537771) designed complementary to all coding exons of 111 myeloid driver-genes.

Eliminating germline events and technical artifacts using tumor comparator

Using a synthetic dataset, we profiled the error rates of several methods that use the matched tumor as a comparator to eliminate germline events and false positive calls (artifacts).

We simulated pairs of observed variant allele fractions in the blood and the tumor as follows:

Let f_b be the true variant allele fraction in blood, f_t be the true variant allele fraction in tumor and c be the level of blood contamination in the tumor and $r \in \{0,1\}$ be an indicator for whether the variant is real ($r=1$) or artifact ($r=0$). Let v_b be the observed VAF in the blood, v_t be the observed VAF in tumor and d be the sequencing depth in both blood and tumor. For convenience, d is fixed to be 500 as per the typical coverage for IMPACT sequencing panels.

A called mutation m can be either be true CH (a somatic mutation in the blood), an artifact, or a germline mutation. If m is a real CH mutation, then we would expect the tumor VAF to be a product of the amount of blood contamination in the tumor and the true VAF in the blood, $f_t = cf_b$. If m is an artifact or a germline mutation, we would expect the tumor VAF to be same as the blood VAF, namely $f_t = f_b$. v_t is expected to follow a binomial distribution based on the

sequencing depth d and true VAF in the blood and tumor respectively. Thus, the observed blood VAF can be modeled by $v_b \sim \text{Bin}(d, f_b)$ while the observed tumor VAF can be modeled by $v_t \sim \text{Bin}(d, c, f_b)$. We simulated the observed blood and tumor VAFs for real and artifactual mutations under a range of blood contamination levels ($c = \{0.05, 0.1, \dots, 0.5\}$) and true blood VAFs ($f_b = \{0.02, 0.04, \dots, 0.2\}$). Using this synthetic dataset, we evaluated two methods (with different threshold parameters) that aim to differentiate real CH variants from non-CH variants using the observed VAFs:

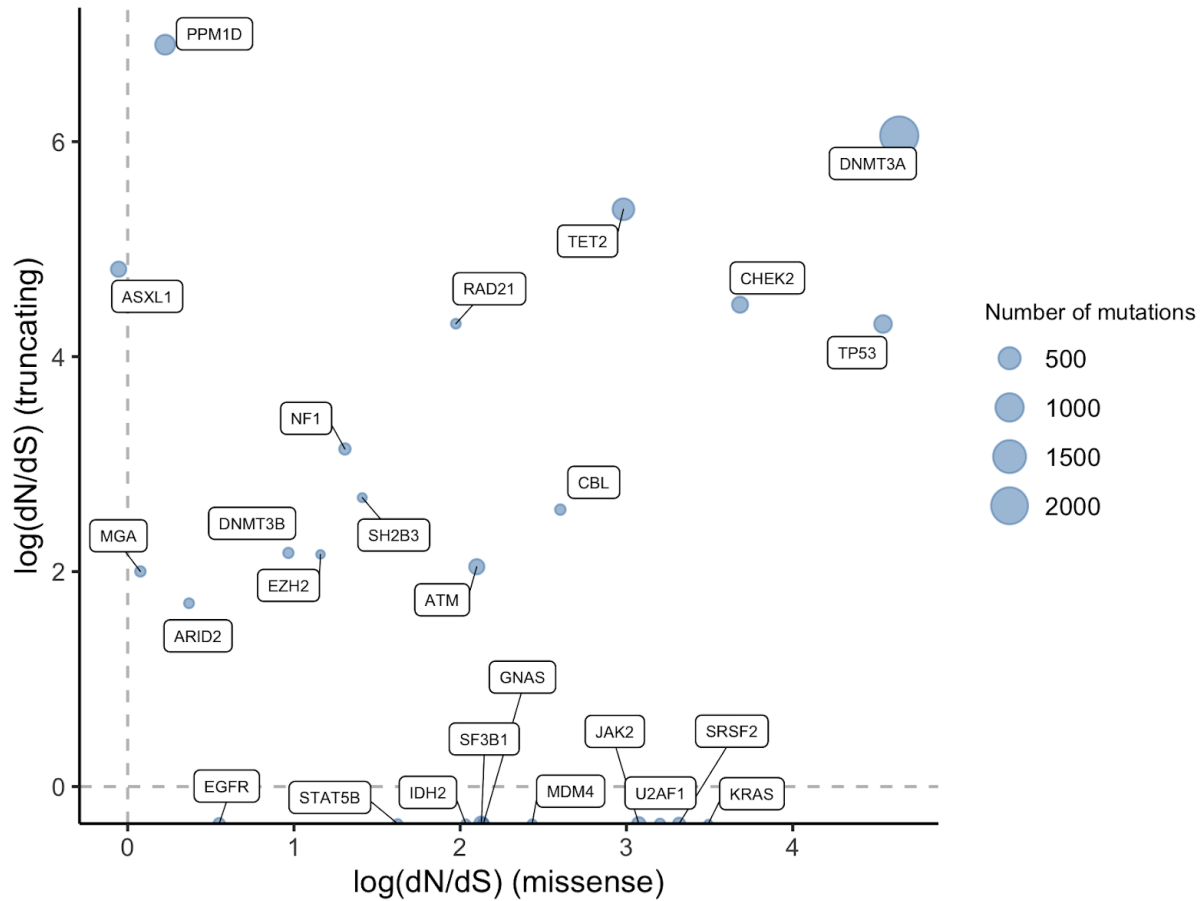
1. Blood-tumor Ratio: Predict mutation is real if $v_b / v_t \geq C$ otherwise consider it an artifact. We evaluated a range of cutoffs for $C \{1, 1.5, 2, 3, 4\}$.
2. Binomial test: Predict mutation is real if $p < 0.05$ from a binomial test with the null hypothesis of $v_b = v_t$

The predictions by each method were evaluated against the true mutation types that gave rise to the data points, and were classified as true positive (TP), false positive (FP), true negative (TN), and false negative (FN). The overall precision of various methods/cutoffs were calculated as $TP / (TP + FP)$ and its recall as $TP / (TP + FN)$ (Supplementary Figures 13 and 14).

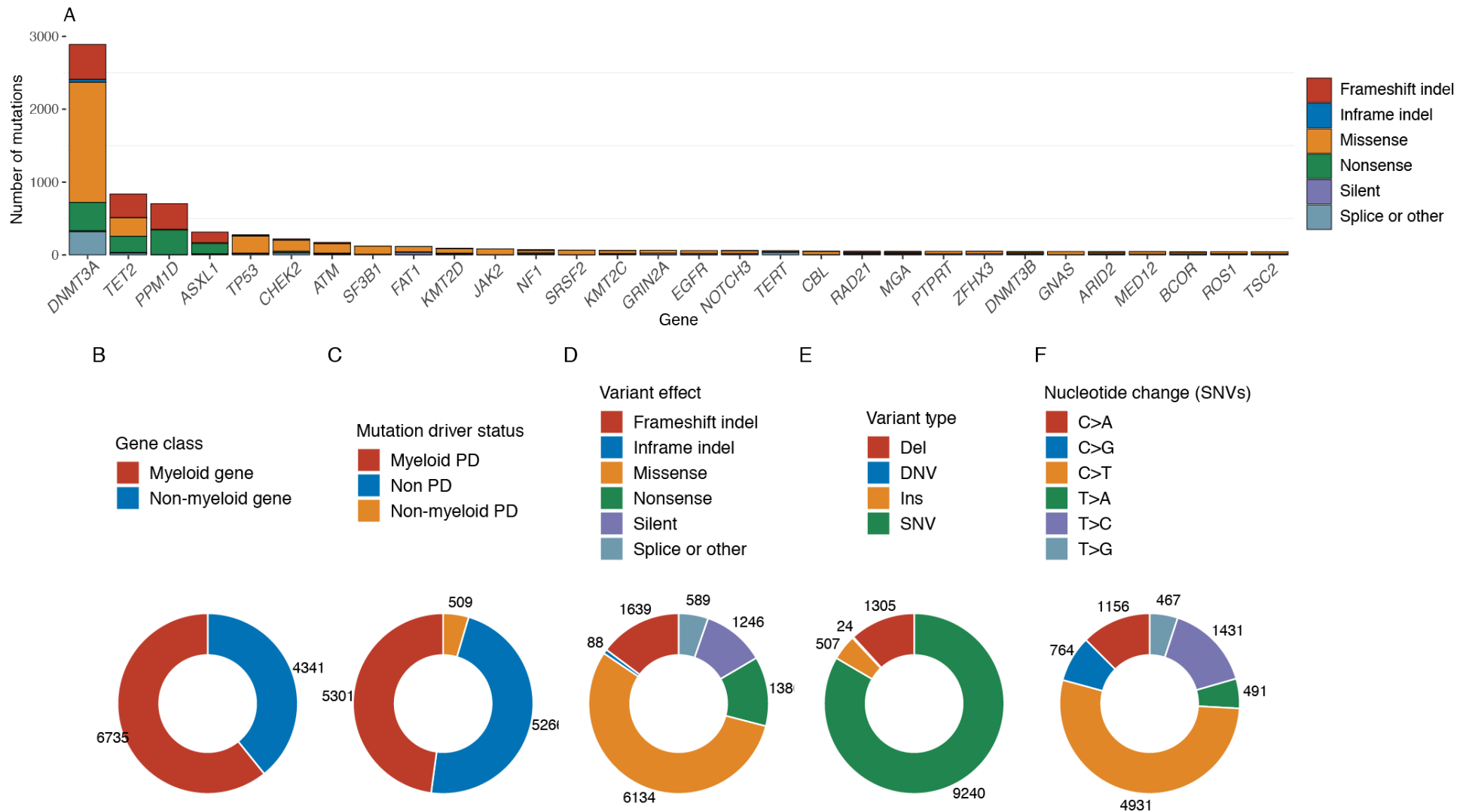
Since we expect most CH mutations to have a true variant allele frequency of less than 10% and since we expect most solid tumors to a range of contamination levels with leukocytes (but generally less than 20%), based on our simulations we used v_b / v_t cutoff of two. However, in the situation where a lymph node with metastatic disease was chosen as the source for tumor material, a high level (greater than 30%) of leukocyte contamination could be present in some cases. Thus when the biopsy site for the tumor was a lymph node, we used v_b / v_t cutoff of 1.5.

REFERENCES

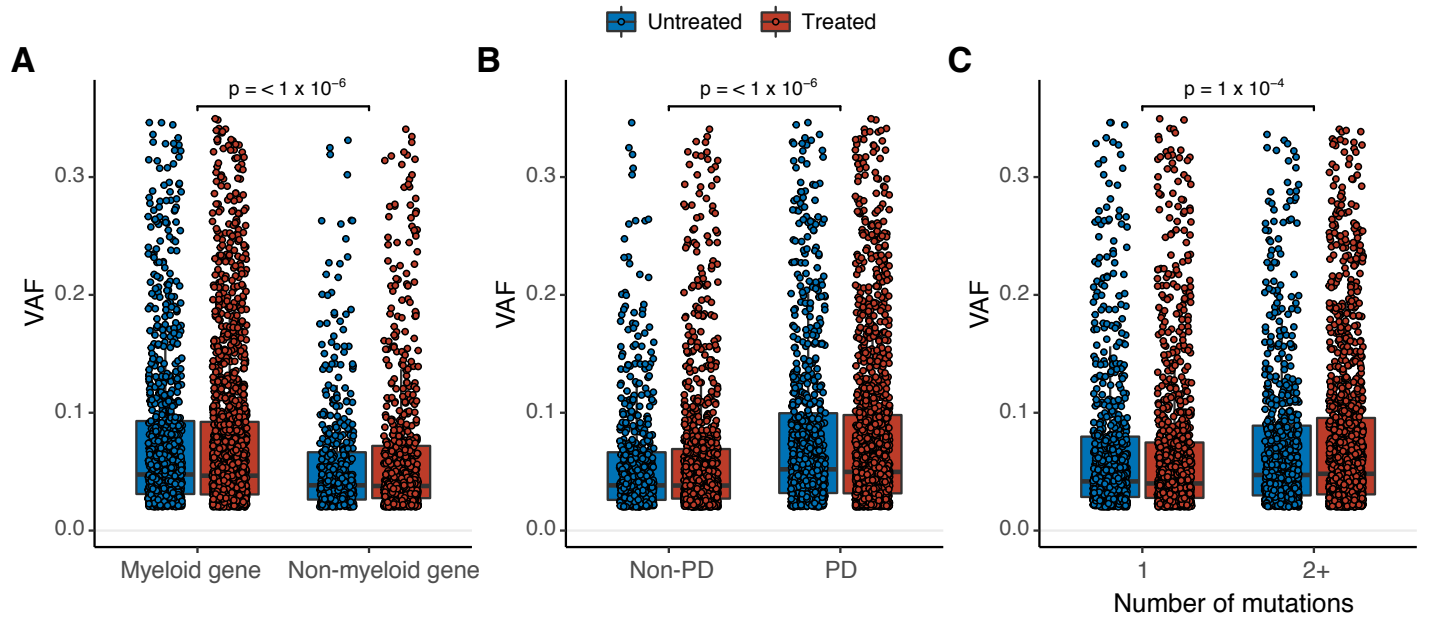
1. Tucker, M. A. *et al.* Leukemia After Therapy With Alkylating Agents for Childhood Cancer. *JNCI: Journal of the National Cancer Institute* vol. 78 459–464 (1987).
2. Chan, T. A., Hristov, B. & Powell, S. N. Radiation Biology for Radiation Oncologists. *Clinical Radiation Oncology* 15–61 (2017) doi:10.1002/9781119341154.ch2.
3. Gillis, N. K. *et al.* Clonal haemopoiesis and therapy-related myeloid malignancies in elderly patients: a proof-of-concept, case-control study. *Lancet Oncol.* **18**, 112–121 (2017).
4. Takahashi, K. *et al.* Preleukaemic clonal haemopoiesis and risk of therapy-related myeloid neoplasms: a case-control study. *Lancet Oncol.* **18**, 100–111 (2017).
5. Gibson, C. J. *et al.* Clonal Hematopoiesis Associated With Adverse Outcomes After Autologous Stem-Cell Transplantation for Lymphoma. *J. Clin. Oncol.* **35**, 1598–1605 (2017).
6. Young, A. L., Tong, R. S., Birmann, B. M. & Druley, T. E. Clonal haematopoiesis and risk of acute myeloid leukemia. *Haematologica* (2019) doi:10.3324/haematol.2018.215269.
7. Young, A. L., Challen, G. A., Birmann, B. M. & Druley, T. E. Clonal haematopoiesis harbouring AML-associated mutations is ubiquitous in healthy adults. *Nat. Commun.* **7**, 12484 (2016).
8. Abelson, S. *et al.* Prediction of acute myeloid leukaemia risk in healthy individuals. *Nature* **559**, 400–404 (2018).
9. Riboli, E. The EPIC Project: rationale and study design. European Prospective Investigation into Cancer and Nutrition. *International Journal of Epidemiology* vol. 26 6S–14 (1997).



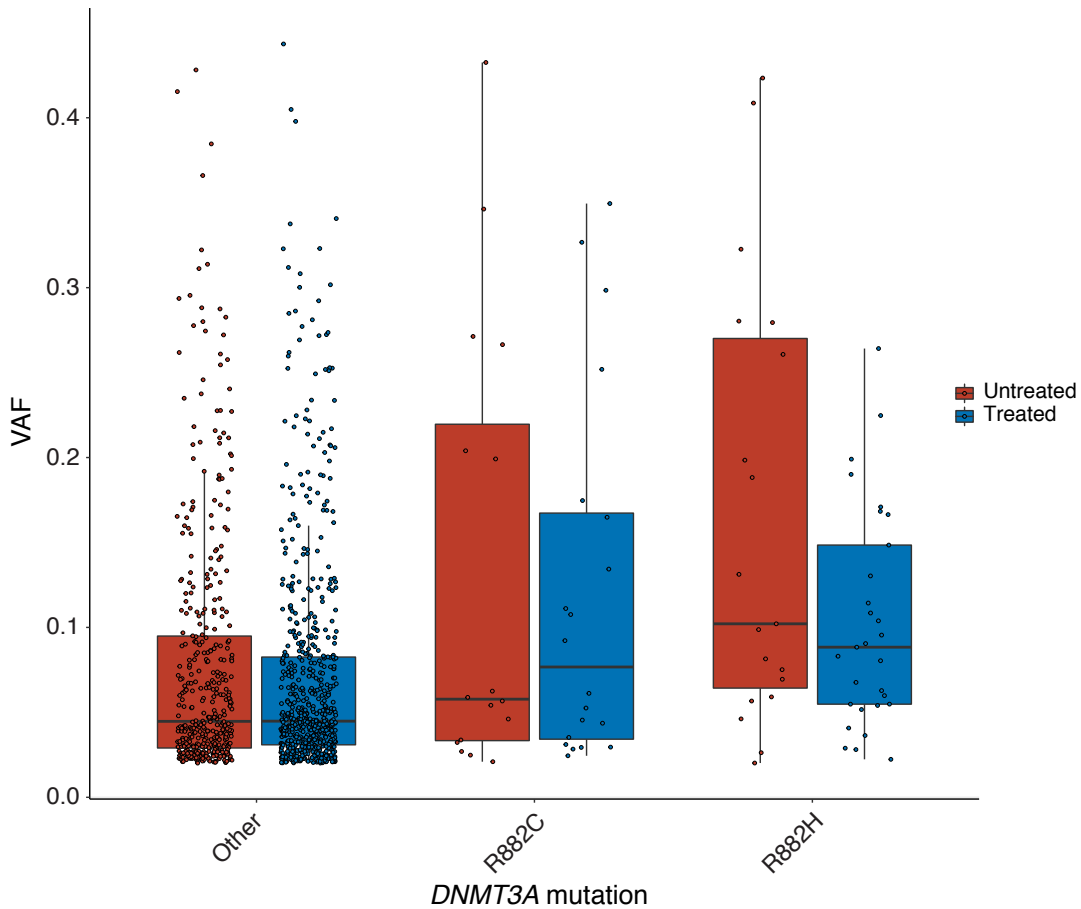
Supplementary Figure 1. Quantification of the extent of natural selection by gene in clonal hematopoiesis using a dN/dS method. Using the dNdScv method (see Methods), we quantified the dN/dS ratios for missense and nonsense and essential splice mutations (truncating) at the level of individual genes. This includes CH mutations from 24,146 solid tumor patients. Shown are the dN/dS ratios for genes mutated at least 25 times showing evidence of significant selection. $\log(dN/dS) < 0$ provides evidence of negative selection and $\log(dN/dS) > 0$ provides evidence of positive selection.



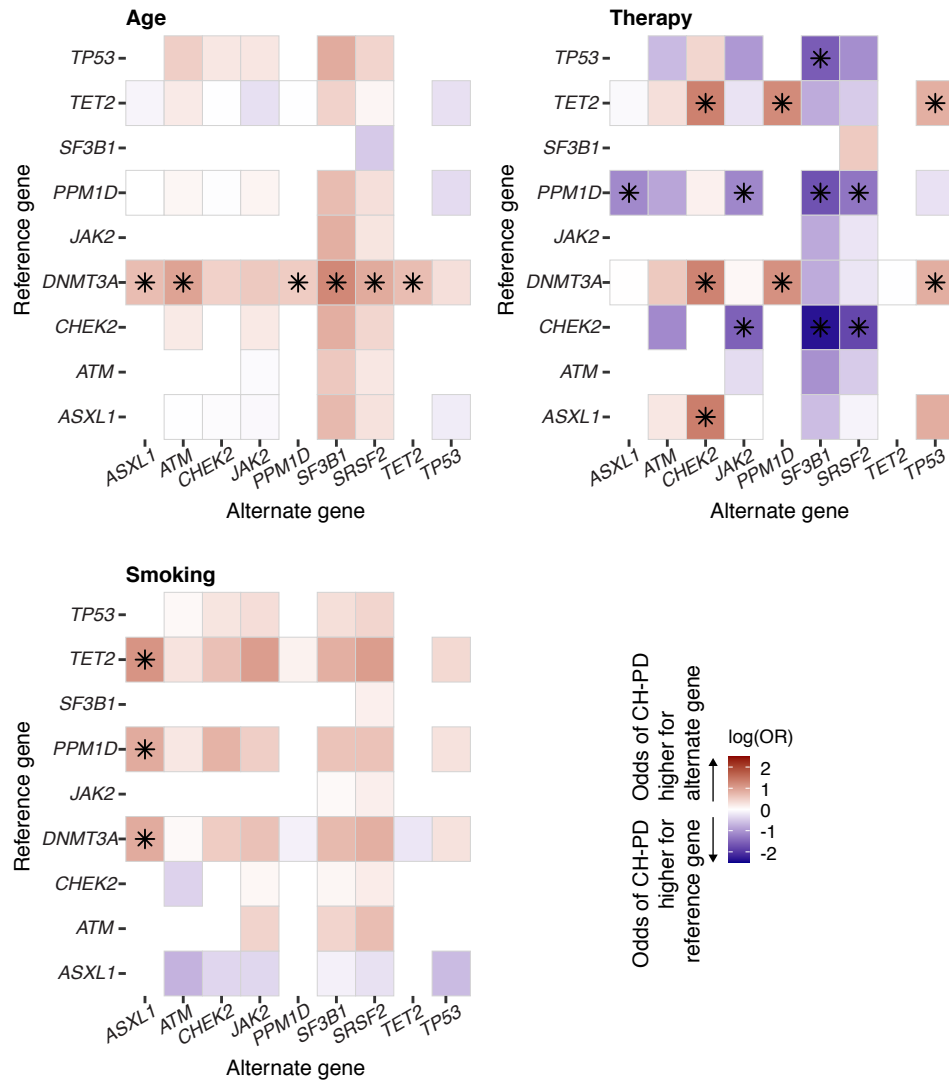
Supplementary Figure 2. Mutational characteristics of CH in 24,146 solid tumor patients. (A) Number of mutations observed in the 30 most common genes. (B) Proportion of mutations in a myeloid gene and those not in a myeloid gene. (C) Proportion of mutations considered to be a possible driver of myeloid neoplasms (myeloid PD), a driver of non-myeloid neoplasms (non-myeloid PD) and those not considered to be a possible cancer driver. (D) Proportion of mutations by functional effect. (E). Proportion of deletions (DEL), insertions (INS) or SNVs. (F). Proportion of SNVs with specific nucleotide.



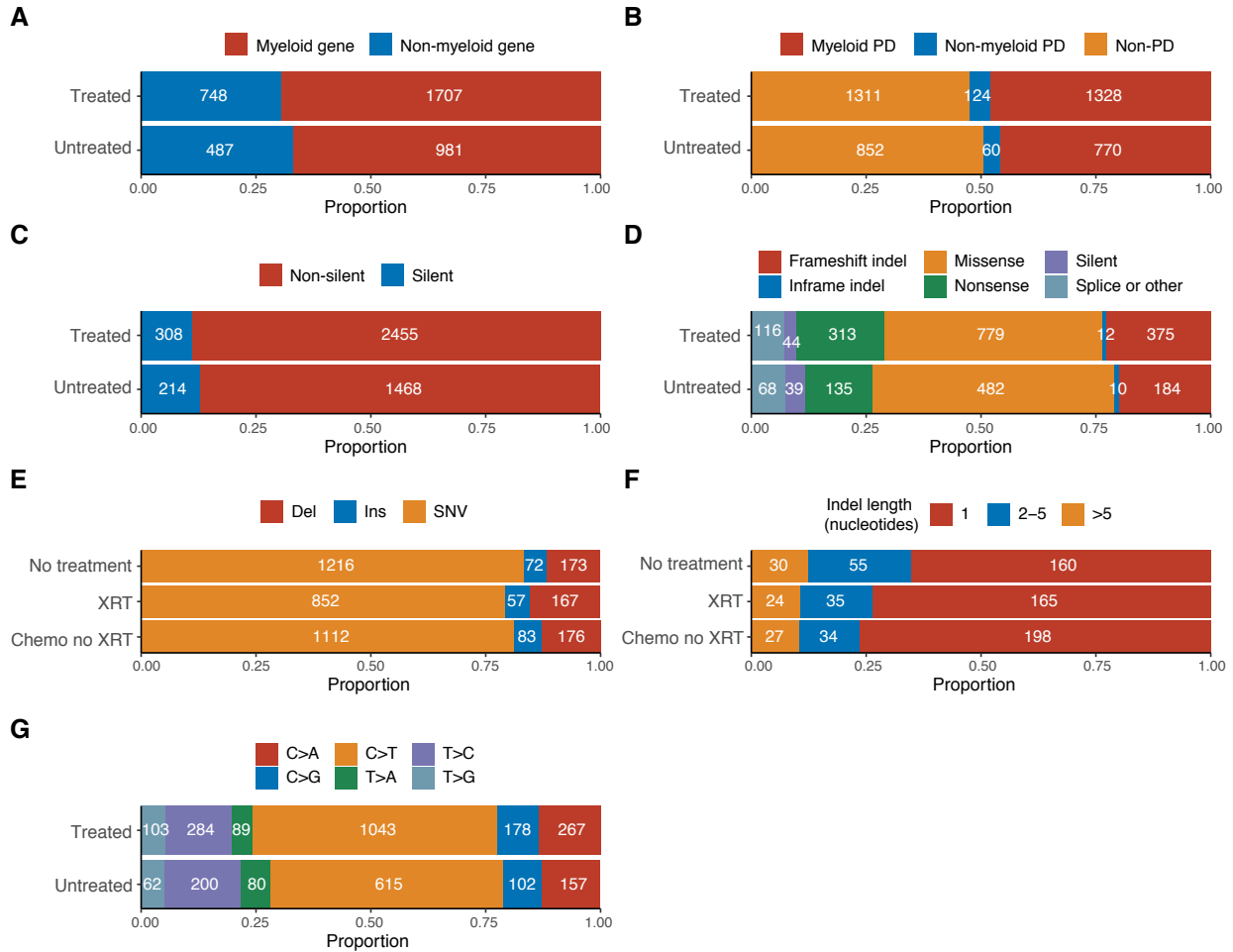
Supplementary Figure 3. Relationship between variant allele fraction (VAF) and CH mutational features. Differences in VAF between: (A) genes recurrently mutated in myeloid neoplasms (myeloid gene) vs. those not implicated in myeloid disease (non-myeloid gene), (B) variants thought to be putative cancer drivers (PD) vs. variants not known to be cancer drivers (non-PD) and (C) individuals with 1 vs. 2+ mutations. P-values were calculated from generalized estimating equations testing for associations between VAF and mutational features adjusted for age, sex, race, smoking history and exposure to oncologic therapy accounting for the within-subject correlation in VAF. $n=10,138$. Boxplots display interquartile ranges.



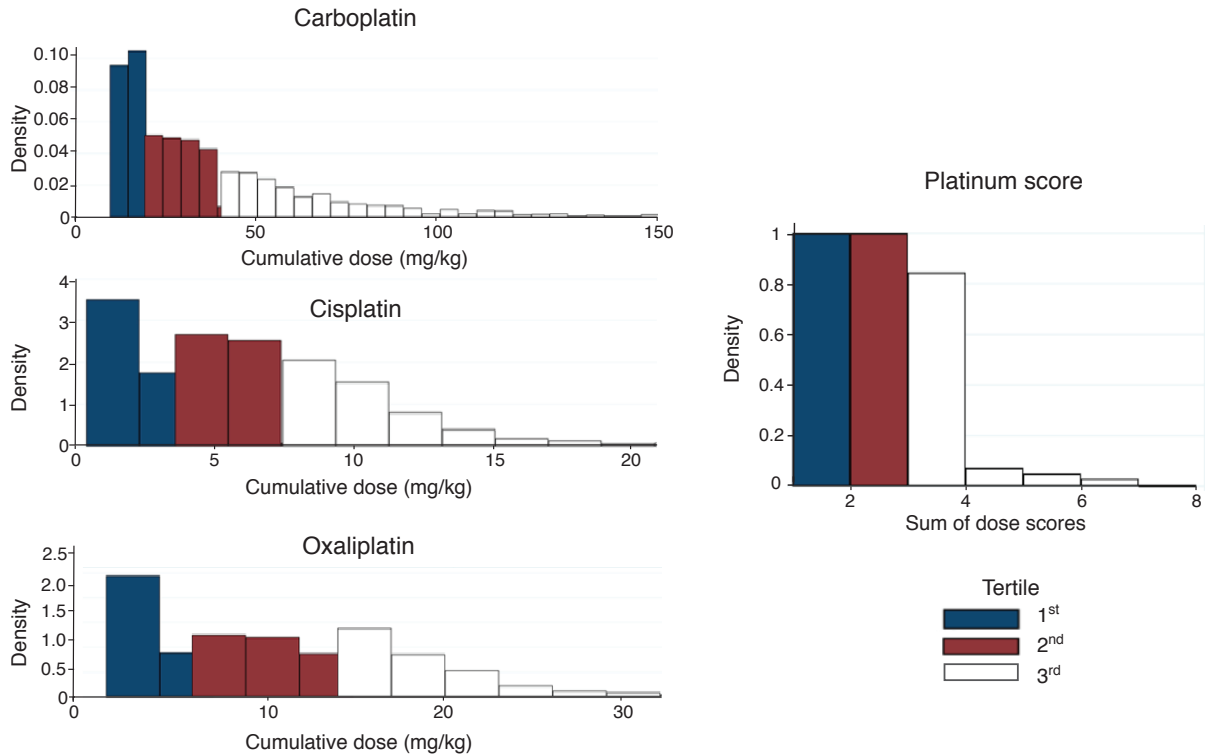
Supplementary Figure 4. Relationship between variant allele fraction (VAF) and *DNMT3A* mutations. p-values were calculated using generalized estimating equations adjusted for age, sex, race, smoking history and exposure to oncologic therapy accounting for the within-subject correlation in VAF. **, p-value 0.01; ***, $p < 1 \times 10^{-6}$, respectively). $n=10,138$. Boxplots display interquartile ranges.



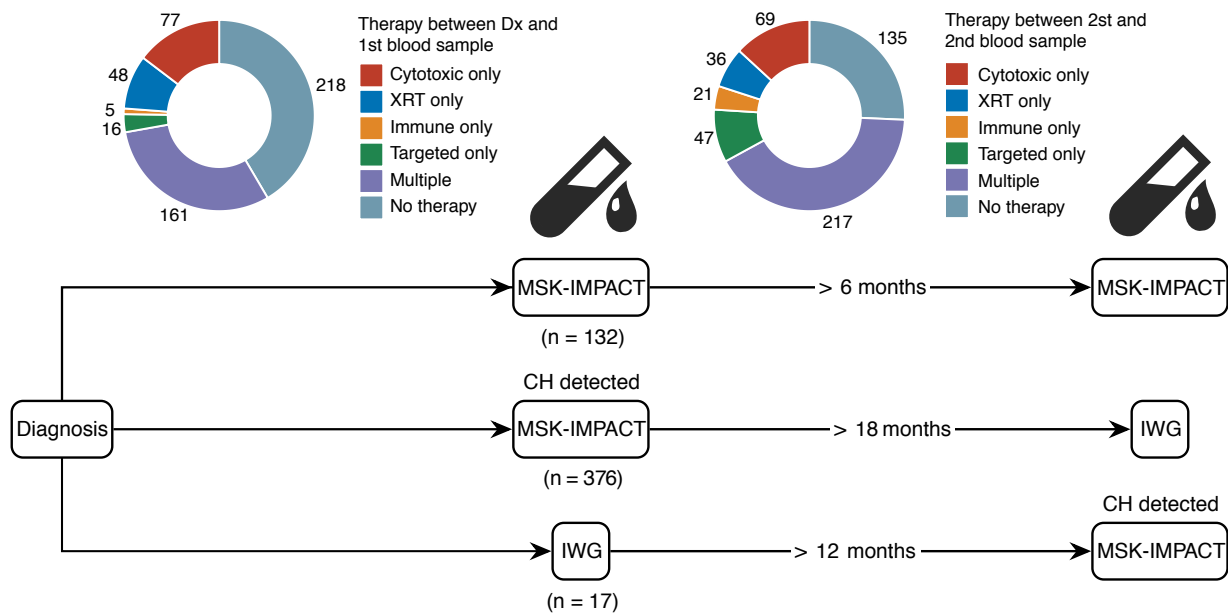
Supplementary Figure 5. Relative odds of CH in specific genes by clinical characteristics. Heatmap of the natural log of the odds ratio for CH-PD in the alternate gene compared to the reference gene from multivariable logistic regression. All combinations (N=45) of the nine most common genes were included. The more common gene from the combination used as the reference. All models were adjusted for age, race, smoking, gender and therapy exposure prior to blood draw. * q (FDR-corrected p-values) < 0.05.



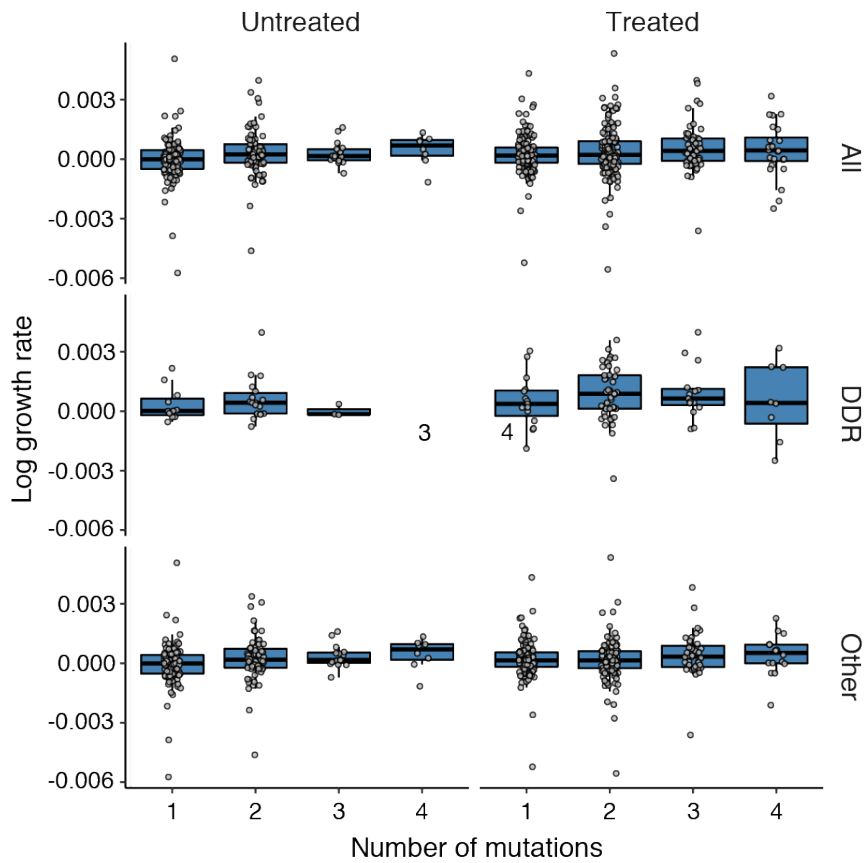
Supplementary Figure 6. Mutational characteristics of CH and prior exposure to cancer therapy in patients with solid tumors. Among patients who received any cancer treatment prior to blood draw for mutational testing (treated) and those who did not receive therapy prior to blood draw (untreated) we compared proportions of: (A) Mutations in a hypothesized myeloid neoplasm driver gene (myeloid gene) vs. those in a gene not known to be a driver of myeloid neoplasms (non-myeloid gene). (B) Mutations considered to be a possible driver of myeloid neoplasms (myeloid PD), a driver of non-myeloid neoplasms (non-myeloid PD) vs. those not considered to be a possible cancer driver (non-PD). (C) Proportion of non-synonymous (non-silent) vs. synonymous (silent) mutations. (D). Proportion of mutations within major functional effect categories. (E) Proportion of deletions (Del), insertions (Ins) or single nucleotide variants (SNV). (F) Proportion of insertions or deletions by the nucleotide length of the alteration. (G) Proportion of SNVs with specific nucleotide changes. n = 10,138.



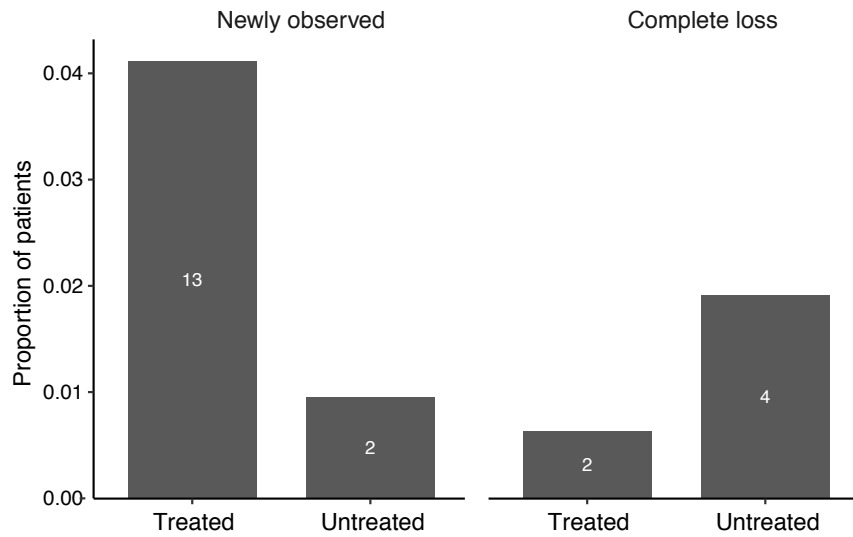
Supplementary Figure 7. Calculation of cumulative exposure for therapy subclasses. For each drug and for all platinum agents, the total dose per kilogram of body weight received prior to blood draw was summed for each patient. The dose distribution for each agent was divided into tertiles and the patient’s dose was assigned a score based on tertile.



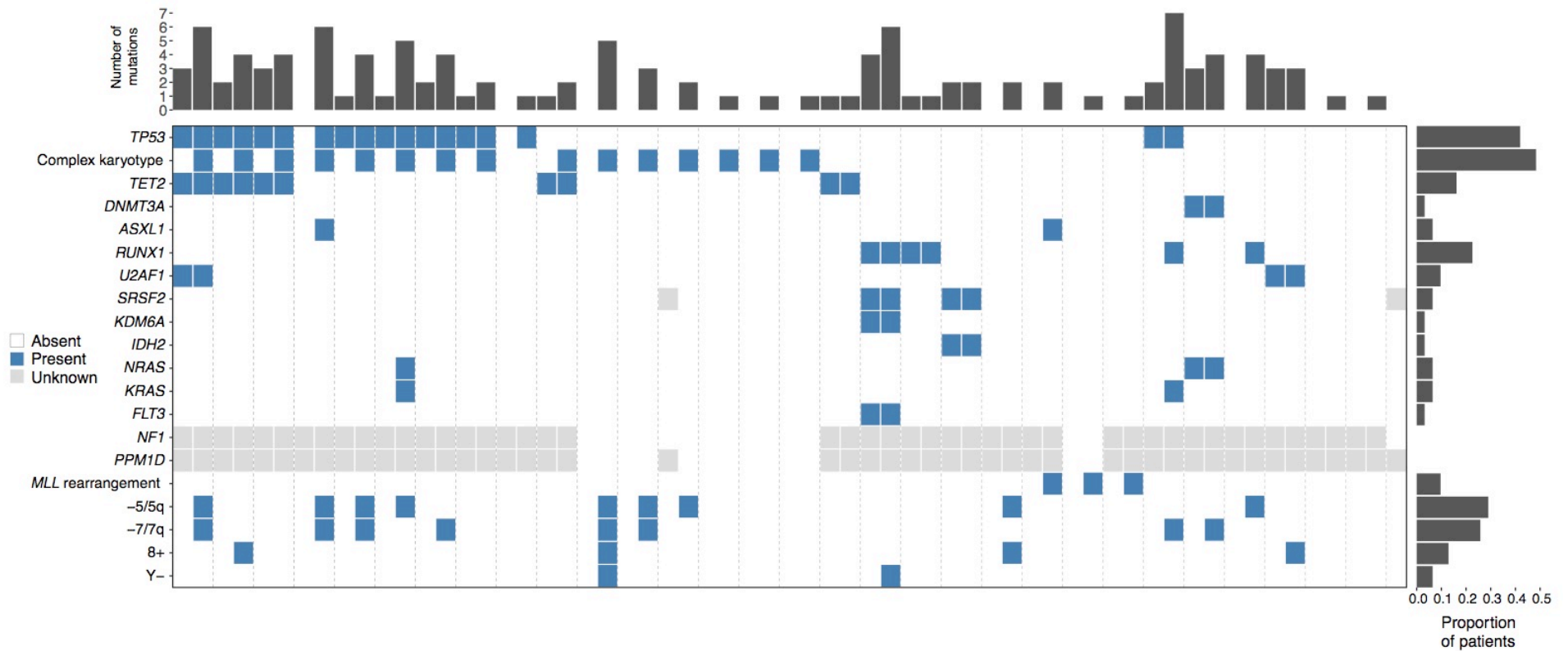
Supplementary Figure 8. Overview of serial samples included in the study relative to MSK-IMPACT testing. Serial samples included in the study, of which at least one was analyzed by MSK-IMPACT testing. Top, treatment received; bottom, timing and type of genomic analysis. n=525.



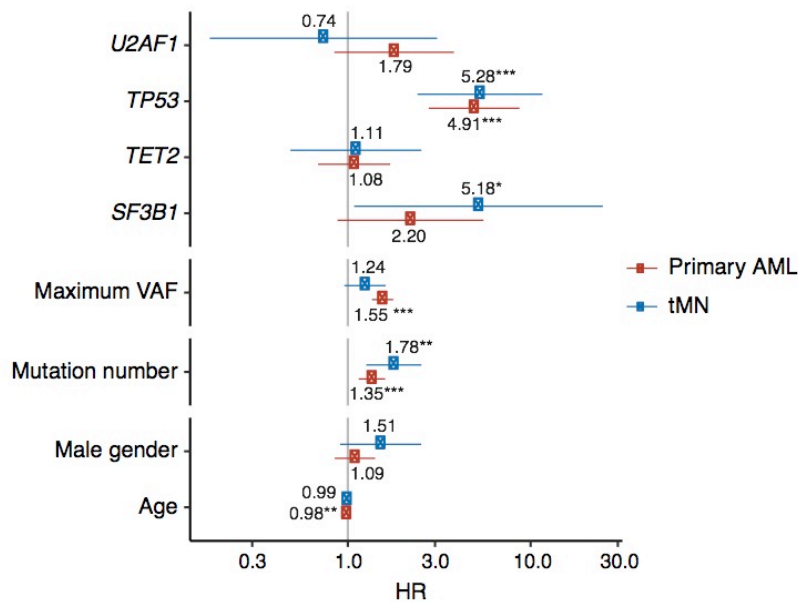
Supplementary Figure 9. Growth rate of CH mutations vs. mutation number. Growth rates for each mutation during follow-up according to the total number of mutations in that individual stratified by receipt of therapy in 525 individuals. Regression using generalized estimating equations was used to test for trend toward increasing growth rate with mutation number among subjects with clonal hematopoiesis adjusted for age, gender, treatment and smoking accounting for correlation between the VAF of mutations in the same person, yielding a p -trend=0.03. Boxplots display interquartile ranges.



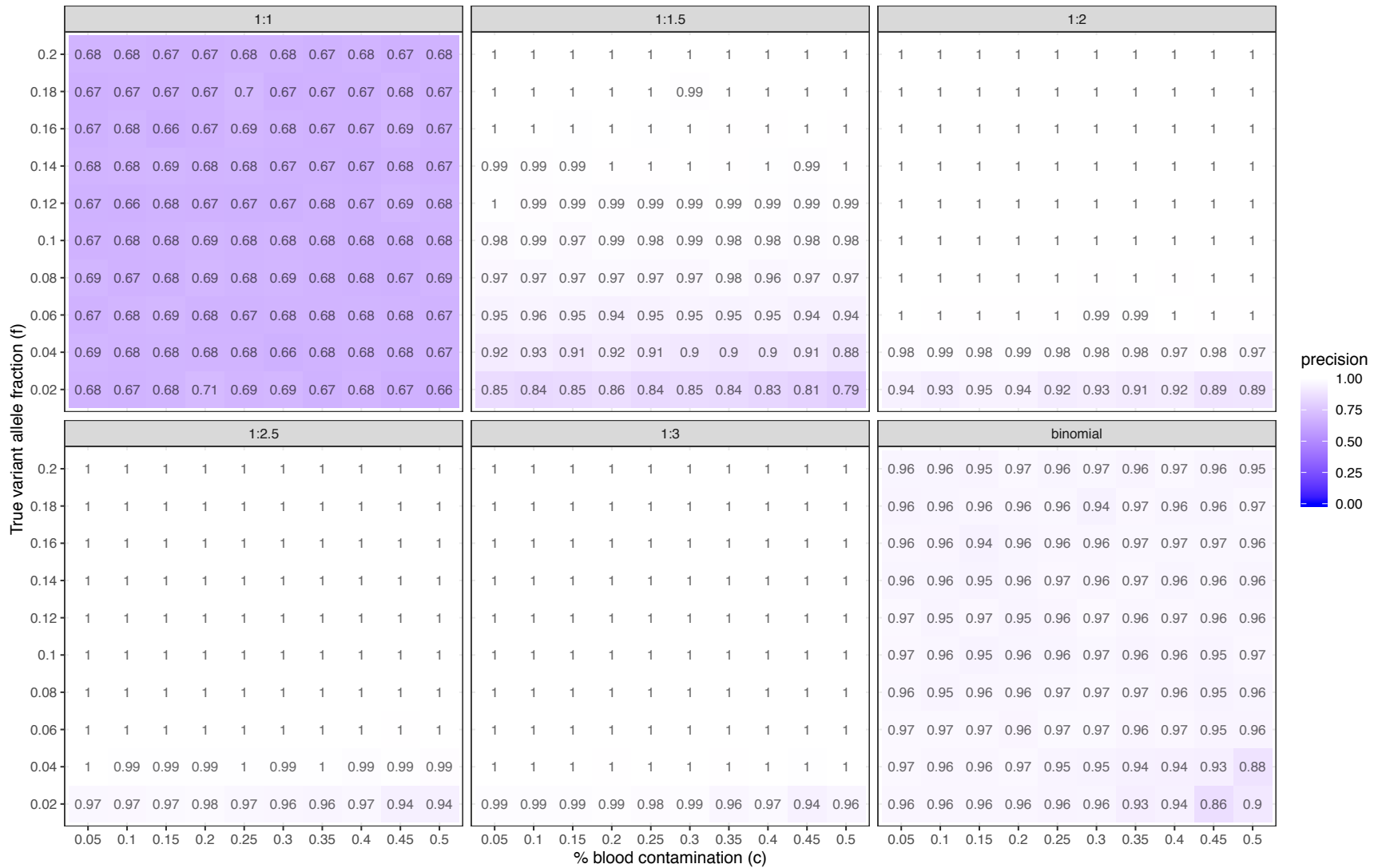
Supplementary Figure 10. Proportion of patients who gained or lost a mutation during follow-up stratified by receipt of therapy. Newly observed, no initial read, VAF $\geq 2\%$ at follow-up; complete loss, initial VAF $\geq 2\%$, no read at follow-up.



Supplementary Figure 11. Mutation landscape in tMN cases with at least one genetic alteration present at the time of tMN diagnosis. Out of 35 samples with paired pre- and tMN samples, 34 had at least one genetic alteration and are displayed here. N01, pre-tMN sample; -tMN, sample attained at time of tMN diagnosis. Chromosomal abnormalities were not evaluated at the time of pre-tMN testing. Genes included in this analysis are listed in Supplemental Table 5.



Supplementary Figure 12. Risk of myeloid malignancy by clinical and mutational characteristics comparing studies for tMN in solid tumor patients and AML risk in healthy individuals. Hazard ratios and 95% confidence intervals from multivariable Cox regression for including CH mutational characteristics. All models were adjusted for age and gender and stratified by study center. Patients with solid tumors, n=9,437; healthy individuals, n=1,072.



Supplementary Figure 13. Precision of CH calling by simulation. Precision for discrimination of true CH calls from artifacts using a range of cutoffs (1:1, 1:1.5, 1:2, 1:2.5, 1:3) for the ratio of VAF in blood to VAF in tumor and a binomial test of the null hypothesis for an equal VAF in blood and tumor.



Supplementary Figure 14. Recall of CH calling by simulation. Recall for discrimination of true CH calls from artifacts using a range of cutoffs (1:1, 1:1.5, 1:2, 1:2.5, 1:3) for the ratio of VAF in blood to VAF in tumor and a binomial test of the null hypothesis for an equal VAF in blood and tumor.